Quantitative correlation between the local coercivity variation and magnetization reversal dynamics in Co/Pd multilayer thin films

Hyuk-Jae Jang
School of Physics and Astronomy, University of Minnesota, 116 Church Street, SE Minneapolis, Minnesota 55455

Sug-Bong Choe and Sung-Chul Shin[a)]
Department of Physics and Center for Nanospinics of Spintronic Materials, Korea Advanced Institute of Science and Technology, Daejeon 305-701, Korea

We report the existence of a quantitative correlation between magnetization reversal dynamics and spatial variation of the local coercivity, ΔH_C, in Co/Pd multilayer thin films. The ΔH_C was directly probed by measuring hysteresis loops on spatially resolved local regions by means of a magneto-optical microscope magnetometer and magnetization reversal dynamics was characterized by analyzing the wall-motion speed V and the nucleation rate R. We found a linear relationship between $\log(V/R)$ and $\log(\Delta H_C)$, where a small variation of the local coercivity results in a large V/R showing wall-motion dominant reversal behavior. A Monte Carlo simulation considering magnetic nonuniformity well predicts the observed experimental relationship. © *2003 American Institute of Physics.* [DOI: 10.1063/1.1577220]

Co/Pd multilayer thin films are of continuing interest for potential applications to high-density perpendicular magnetic and magneto-optical recording media due to their large magnetic anisotropy and Kerr rotation.[1] Because the magnetization reversal process basically involves writing and erasing data, magnetization reversal dynamics study in this system is very important for achieving high performance of technological applications as well as for fundamental understanding of the reversal process.[2–4] Recently, advanced magnetic imaging techniques have provided direct evidence of the contrasting magnetization reversal dynamics between wall-motion dominant and nucleation dominant processes in this system.[4,5] Macroscopic magnetic properties have been examined to explain the intrinsic origin of the contrasting reversal dynamics within the context of a micromagnetic description.[5–7] Local magnetic variation due to structural irregularities has also been studied as another possible origin.[8,9] Among local magnetic properties, the local coercivity has been considered as one of the most important parameters contributing to reversal dynamics and recording noise, because its fluctuation may cause an inhomogeneity in domain shape and size.[9,10] Therefore, it is imperative to understand how the local coercivity variation affects reversal behavior. However, the effect of the local coercivity variation on contrasting magnetization reversal dynamics has not yet been quantitatively investigated.

In this work, we quantitatively probed the local coercivity variations of Co/Pd multilayer films from simultaneous measurements of the local Kerr hysteresis loops by means of a magneto-optical microscope magnetometer (MOMM).[11] The results were then compared with magnetization reversal behavior investigated at *the precisely same* positions of the

samples. We present here the observations of the quantitative correlation between the local coercivity variation and magnetization reversal dynamics together with a micromagnetic simulation to explain the experimental observations.

For this study, we prepared multilayered samples of $(2 \text{ Å Co/11 Å Pd})_n$ with varying number of bilayer repeats n from 3 to 20. Reversal dynamics in a Co/Pd multilayer system was reported to sensitively change from a wall-motion dominant process to a nucleation dominant process with an increase of either the number of repeats[4] or the Co-sublayer thickness.[5] We chose to vary the number of repeats n because with increasing n, the local structural irregularities were expected to increase due to the possible accumulation of lattice misfits, residual stress, and other defects at interfaces during the deposition process under a high vacuum. This in turn was expected to sensitively affect the local coercivity variation. The individual bilayer thickness was kept constant to prevent substantial changes of macroscopic magnetic properties.

Samples were prepared on glass substrates by electron-beam evaporation under a base pressure of 2.0×10^{-7} Torr at ambient temperature. The layer thickness was controlled within 4% accuracy. Low-angle x-ray diffraction studies using Cu $K\alpha$ radiation revealed that all samples had distinct peaks indicating the existence of a multilayer structure. All of the samples had perpendicular magnetic anisotropy and showed $M-H$ hysteresis loops of unit squareness. As expected, the macroscopic magnetic properties such as saturation magnetization were confirmed to be the same within an experimental error for all samples. Hence, possibility of contrasting magnetization reversal behavior caused by different macroscopic magnetic properties among the samples was minimized. A homemade MOMM system was used for the local hysteresis loop measurements as well as the real-time magnetization reversal image analysis by utilizing the

---

[a)]Electronic mail: shin@kaist.ac.kr

10143
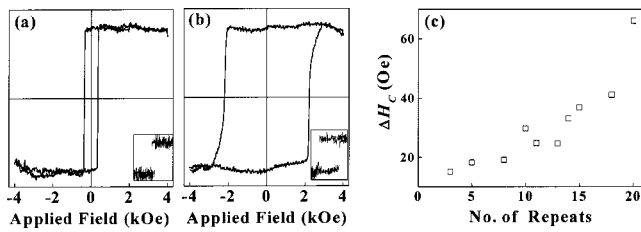
FIG. 1. The hysteresis loop of $(2\ \text{Å Co}/11\ \text{Å Pd})_n$ multilayer samples with (a) $n=3$ and (b) $n=18$, respectively, on a sample area of $32.0 \times 25.6\ \mu\text{m}^2$. The inset images show the typical hysteresis loop measured on a local region of $0.98 \times 0.98\ \mu\text{m}^2$. The standard deviation ΔH_C of the local coercivity variation of $(2\ \text{Å Co}/11\ \text{Å Pd})_n$ samples is plotted in (c).

magneto-optical polar Kerr effect. Details of this system have been described elsewhere.[11]

In Fig. 1, we illustrate hysteresis loops measured on a $32.0 \times 25.6\ \mu\text{m}^2$ region of the samples having [Fig. 1(a)] $n=3$ and [Fig. 1(b)] $n=18$, respectively, together with the typical shape of local hysteresis loops measured on a local region of $0.98 \times 0.98\ \mu\text{m}^2$ in the inset of Figs. 1(a) and 1(b). Note that the local hysteresis loops were measured simultaneously for every local region of $0.98 \times 0.98\ \mu\text{m}^2$ at ambient temperature under a sweeping rate of 10 Oe/s for each sample. It is worthwhile to note that the hysteresis loops from local regions exhibit more square loops than those from larger regions, which can be ascribed to the coercivity variation of square hysteresis loops from local regions since the signal from a large region is the sum of the signals from each local region inside the large region.[10] We measured local coercivities from the local hysteresis loops and then determined the standard deviation ΔH_C. Figure 1(c) is a plot of local coercitvity variation ΔH_C with respect to n. It is clearly seen in Fig. 1(c) that ΔH_C sensitively increases with increased n. A larger ΔH_C of the thicker film can be considered to result from a larger density of microstructural irregularities with increasing n.[9]

Using the MOMM system, magnetization reversal dynamics were also investigated via time-resolved observation of domain evolution patterns at *precisely the same* position of the samples studied in Fig. 1. Each sample was first saturated by applying a magnetic field much larger than the saturation field and then magnetization reversal was triggered by applying a constant reversing magnetic field of about 90% of the mean coercivity.

Reversal behavior in these samples was found to sensitively change from wall-motion dominant to nucleation dominant with increasing n. The inset images of Fig. 2 show the typical domain patterns at about 50% reversal for the samples of $n=3$ and 18, respectively. The domain reversal pattern of $n=3$ indicates a gradual expansion of domains via the continuous wall-motion process from a single nucleation site, while the disorderly pattern of $n=18$ manifests an anisotropic jutting out of domain sprouts adjacent to the existing domain boundary via the nucleation process. The contrasting reversal behavior is ascribed to a counterbalancing between the wall-motion and nucleation processes.[3]

Contrasting magnetization reversal behavior is known to be characterized by the reversal ratio V/R, where V and R
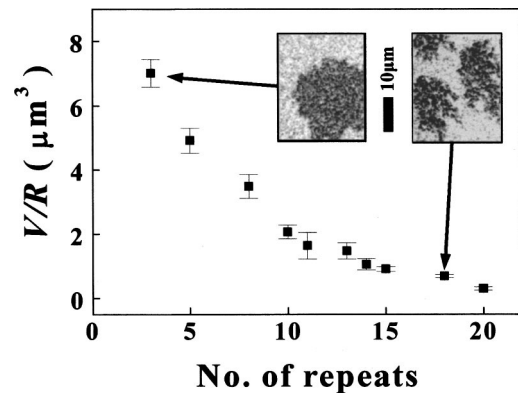
FIG. 2. The reversal ratio V/R vs number of repeats n of $(2\ \text{Å Co}/11\ \text{Å Pd})_n$ samples. The inset images illustrate the domain reversal patterns of the samples with $n=3$ and 18.

are the wall-motion speed and nucleation rate, respectively: Magnetization reversal behavior changes from nucleation dominant to wall-motion dominant with an increasing of the reversal ratio.[4,12] In our study, from the measured domain area and domain boundary length of each image, V and R were quantitatively determined by utilizing an analysis method proposed by Choe and Shin.[13] As expected in the domain patterns of the samples, V/R decreases with increasing n as shown in Fig. 2.

Interestingly, the reversal ratio V/R was found to be closely related with ΔH_C. For a quantitative analysis of the correlation, in Fig. 3, we plot V/R versus ΔH_C for the $(2\ \text{Å Co}/11\ \text{Å Pd})_n$ samples, where the x axis is ΔH_C in logarithmic scale and the y axis is V/R in logarithmic scale. In Fig. 3, we see that V/R is truly correlated with ΔH_C and the correlation can be well fitted by a simple analytic function given by

$$\log(V/R) = \alpha \log(\Delta H_C) + \beta, \tag{1}$$

where α and β are the fitting parameters. The values of α and β are determined to be -2.25 ± 0.12 and 3.48 ± 0.17, respectively. We would like to stress that Eq. (1) well characterizes the general relation between V/R and ΔH_C for all our Co/Pd multilayer thin films with varying n. A sample having a small ΔH_C reveals wall-motion dominant reversal with a
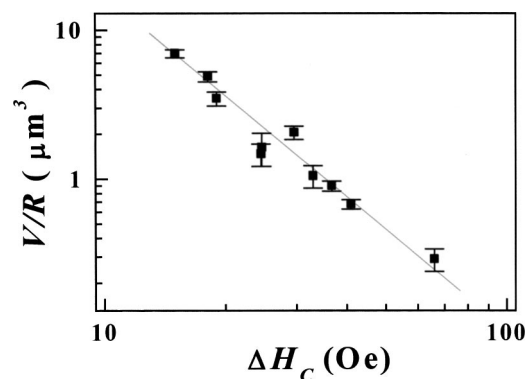
FIG. 3. The correlation between the reversal ratio V/R and the standard deviation ΔH_C of the local coercivity variation. The solid line is the best fit for the correlation.

TABLE I. The values of magnetic parameters used in the simulation.

Magnetic parameters	Values
Uniaxial anisotropy, $\bar{K}_U$	5×10^6 erg/cm^3
Saturation magnetization, M_S	282 emu/cm^3
Wall energy density, σ_ω	2.5 erg/cm^2
Unit-cell volume, V_C	6.93×10^{-18} cm^3
Cell distance, d_c	2×10^{-6} cm
Film thickness, t_f	2×10^{-6} cm

FIG. 4. The reversal ratio V/R vs the relative anisotropy variation δ. The solid line is the best fit for the simulated data for $\delta \geq 1.7\%$. The upper images illustrate the simulated domain reversal patterns at the four different values of δ indicated.

large V/R, while a sample having a large ΔH_C exhibits nucleation dominant reversal with a small V/R. The contrasting magnetization reversal behavior is determined by a counterbalance between the wall-motion and nucleation processes: The wall-motion process in the latter sample is more impeded by the rough spatial irregularity due to its large ΔH_C than that of the former sample having a small ΔH_C. On the other hand, the latter sample has more nucleation sites than the former sample due to its large ΔH_C.

Along with this experiment, a micromagnetic simulation study has been performed to elucidate the results. We used a Monte Carlo algorithm on a two-dimensional lattice of nanosize hexagonal single domain cells with periodic boundary conditions. The magnetic energy E of each cell with the magnetization direction θ from the $+z$ axis is given by

$$E = K_U V_C \sin^2 \theta - M_S V_C (H_z + H_d) \cos \theta$$
$$+ \left(3 - \frac{1}{2} \cos \theta \sum_k \cos \theta_k\right) \frac{d_c t_f \sigma_\omega}{3}, \qquad (2)$$

where t_f is the film thickness, d_c is the distance between the nearest cells, M_S is the saturation magnetization, K_U is the uniaxial perpendicular magnetic anisotropy, σ_ω is the wall energy density of each cell boundary, H_z is the external field, H_d is the demagnetizing field, θ_k is the magnetization direction of the nearest neighbors, and V_C is the volume of a unit cell. Using this model, the domain pattern of the thermally activated reversal process is constructed from each state of individual cells. A detailed explanation of this micromagnetic model is described in Ref. 14.

In this model, since the anisotropy is a very structural-sensitive magnetic property,[15] we limit ourselves to choosing a spatial fluctuation in the uniaxial perpendicular anisotropy as the only parameter reflecting the structural nonuniformity. This means that we assume that ΔH_C is proportional to the anisotropy fluctuation in this model. The anisotropy distribution $K_U(x,y)$ is chosen to be spatially noncorrelated as well so as to have a Gaussian distribution in magnitude with the standard deviation δ:

$$K_U(x,y) = \bar{K}_U \cdot (1 + \delta \cdot f(x,y)), \qquad (3)$$

where $\bar{K}_U$ is the mean value of anisotropy and $f(x,y)$ is the spatially noncorrelated fluctuating function having a unit standard deviation. Typical values of magnetic parameters for Co/Pd multilayered system used in the simulation are listed in Table I.
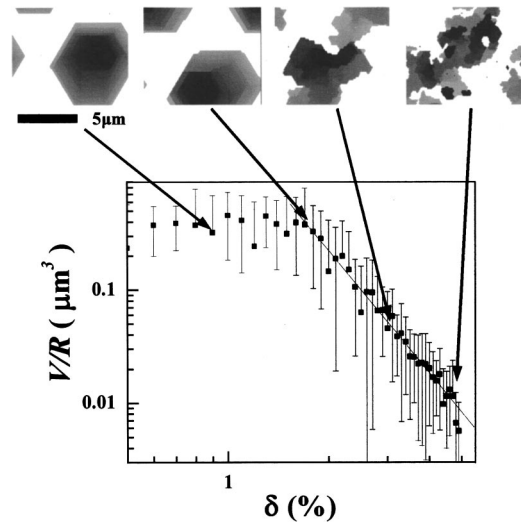
As presented in Fig. 4, V/R is constant until the anisotropy fluctuation δ reaches 1.7%, and then it starts decreasing with an increment of δ. This corresponds to the observation that the domain formation pattern does not change at all before $\delta = 1.7\%$ and after this point, it changes from a wall-motion dominant pattern to a nucleation dominant pattern as δ increases. Also, we see an existence of a linear relationship between $\log(V/R)$ and $\log(\delta)$ after the change of magnetization reversal behavior starts. This theoretical result agrees well with our experimental observations. It should be mentioned that the simulation using the different values of the magnetic properties results in *the same log–log linear* behavior with only variations in the slope and the range of the linear relationship.

[1] S. Hashimoto, Y. Ochiai, and K. Aso, J. Appl. Phys. **67**, 4429 (1990).
[2] J. Ferré, J. P. Jamet, and P. Meyer, Phys. Status Solidi A **175**, 213 (1999).
[3] J. Pommier, P. Meyer, G. Pónissard, J. Ferré, P. Bruno, and D. Renard, Phys. Rev. Lett. **65**, 2054 (1990).
[4] S.-B. Choe, H.-J. Jang, and S.-C. Shin, J. Appl. Phys. **85**, 5651 (1999).
[5] S.-B. Choe and S.-C. Shin, Phys. Rev. B **57**, 1085 (1998).
[6] R. D. Kirby, J. X. Shen, R. J. Hardy, and D. J. Sellmyer, Phys. Rev. B **49**, 10810 (1994).
[7] A. Lyberatos, J. Earl, and R. W. Chantrell, Phys. Rev. B **53**, 5493 (1996).
[8] M. Speckmann, H. P. Oepen, and H. Ibach, Phys. Rev. Lett. **75**, 2035 (1995).
[9] S.-B. Choe and S.-C. Shin, Phys. Rev. B **62**, 8646 (2000).
[10] H.-P. D. Shieh and M. H. Kryder, IEEE Trans. Magn. **24**, 2464 (1988).
[11] S.-B. Choe, D.-H. Kim, Y.-C. Cho, H.-J. Jang, K.-S. Ryu, H.-S. Lee, and S.-C. Shin, Rev. Sci. Instrum. **73**, 2910 (2002); S.-B. Choe and S.-C Shin, Phys. Rev. B **65**, 224424 (2002).
[12] M. Labrune, S. Andrieu, F. Rio, and P. Bernstein, J. Magn. Magn. Mater. **80**, 211 (1989).
[13] S.-B. Choe and S.-C. Shin, Appl. Phys. Lett. **70**, 3612 (1997).
[14] S.-B. Choe and S.-C. Shin, IEEE Trans. Magn. **36**, 3167 (2000).
[15] H. Kronmuller, Phys. Status Solidi B **144**, 385 (1987).